RSC Advances

PAPER

View Article Online
View Journal | View Issue

Cite this: *RSC Adv.*, 2015, **5**, 28332

Hybridization induced fluorescence turn-on of AIEgen–oligonucleotide conjugates for specific DNA detection†

Ruoyu Zhang,[a] Ryan T. K. Kwok,[b] Ben Zhong Tang*[bc] and Bin Liu*[ad]

Received 7th January 2015
Accepted 9th March 2015

DOI: 10.1039/c5ra00322a

www.rsc.org/advances

A bisazide functionalized fluorogen with aggregation-induced emission characteristics (AIEgen) was conjugated to single-stranded oligonucleotides to yield two-armed AIE probes for specific DNA detection. The probes show low emission in aqueous media, which become highly emissive upon hybridization with their complementary strands. The probes are suitable for homogenous sequence-specific DNA detection and are able to discriminate target sequences with even one-base mutation. The signal output can be further enhanced when two probes hybridize to each other to restrict the free rotation of the incorporated AIEgen.

Introduction

Genetic screening reveals that gene mutations are closely related to various human diseases.[1] Specific DNA sequence analyses are routinely used in various fields of biological sciences because they hold the promise of detecting diseases before symptoms appear. Fluorescent techniques, as powerful and simple tools, allow quantification of DNA at very low concentrations.[2] For instance, a variety of organic dyes have been found to selectively bind to DNA with distinguished spectral changes.[3] Typical examples are acridines, cyanines, and phenanthridinium dyes, which intercalate into double-stranded DNA with significant fluorescence enhancement.[4] The prevalence of fluorescent techniques also facilitates real-time quantitative polymerase chain reactions, without the requirement of tedious sample handling.[5]

In various real-time nucleic acid detections, sequence-specific probes show superior performance due to their ability to discriminate perfectly complementary strands from those with mutation points. These probes are generally based on the separation of a fluorophore from a quencher or forbidden energy transfer between a donor and an acceptor to generate significant changes in fluorescence.[6,7] Fluorescent signal changes result from the complementary hybridization between oligonucleotide probe and the target sequence. Molecular beacon[8,9] and binary probes are the two most common designs of hybridization probes, which are very efficient in based mutation detection.[10,11] A variety of probes are developed based on further extension of these principles.[10,12] Besides these organic fluorogens, DNA-like polyaromatic derivatives,[13,14] conjugated polymers,[15,16] and inorganic NPs[17,18] have also been used for sequence-specific nucleic acid detection.

A series of fluorogens with unique aggregation-induced emission (AIE) characteristics have been reported in the past few years, which are non-emissive when molecularly dissolved but highly emissive when aggregated.[19,20] The underlying light-emitting mechanism is ascribed to the restriction of intramolecular motions (RIM) in aggregates which blocks non-radiative decay channel for the excited states to deactivate.[21] Unlike conventional organic fluorogens, the AIE fluorophore are free of aggregation-caused quenching effect and show higher photobleaching resistance.[22] The nature of AIE fluorogens facilitates the development of turn-on bioprobes by taking advantages of aggregation and a wealth of AIE bioprobes have been developed for the detection of proteins,[23–26] DNA[27–29] and other important biomolecules.[30] Previously, AIE-based DNA detections rely on the hydrophobic and electrostatic interactions between anionic DNA and cationic AIE molecules. This mechanism simplifies the development of probes by providing a label-free platform but suffers from interferents with similar electrical properties because of the non-specific nature of electrostatic interactions.

Recently, we have reported a light-up fluorescent probe for homogeneous DNA detection based on an AIE–oligonucleotide conjugate.[31] With one 20-mer oligonucleotide conjugated to a tetraphenylethylene (TPE) derivative, a light-up DNA probe was

[a]*Department of Chemical and Biomolecular Engineering, National University of Singapore, 4 Engineering Drive 4, 117585, Singapore. E-mail: cheliub@nus.edu.sg; Fax: +65-6778-1936; Tel: +65-6516-8409*

[b]*Department of Chemistry, Division of Biomedical Engineering, The Hong Kong University of Science and Technology, Clear Water Bay, Kowloon, Hong Kong, China*

[c]*SCUT-HKUST Joint Research Laboratory, Guangdong Innovative Research Team, State Key Laboratory of Luminescent Materials & Devices, South China University of Technology, Guangzhou 510640, China*

[d]*Institute of Materials Research and Engineering (A*STAR), 3 Research Link, 117602, Singapore*

† Electronic supplementary information (ESI) available. See DOI: 10.1039/c5ra00322a

developed for sequence-specific detection of its complementary strand. The fluorescence of probe is lit up upon hybridization with a perfectly matched strand. The signal-to-background ratio (I/I_0) is ~3.6, which requires further improvement to realize sensitive and specific nucleic acid detection. In this contribution, by tagging two oligonucleotides to one AIE fluorogen, a two-armed DNA probe (AIE–2DNA) is developed, which shows 6.1-fold brighter fluorescence in the presence of the perfect target strand. Furthermore, two AIE–2DNA probes with complementary DNA strands are designed, which can form a longer duplex to further restrict the motions of TPE with enhanced fluorescence, which verifies the fluorescence turn-on mechanism.

Results and discussion

As illustrated in Scheme 1, the fluorescent probe TPE–2DNA$_1$ consists of two components: first, a 20-mer oligonucleotide DNA$_1$ that can hybridize specifically to its complementary strand DNA$_2$. Second, an iconic AIE fluorogen tetraphenylethylene (TPE) which acts as a fluorescent reporter. The probe is synthesized by "click" reaction between oligonucleotide with an alkyne group and bisazide–TPE (TPE–2N$_3$). In this work, the two oligonucleotides endows TPE–2DNA$_1$ with good water-solubility and makes the probe display very weak fluorescence in aqueous media. The hybridization of TPE–2DNA$_1$ with its complementary strand is expected to light up the probe fluorescence as a result of the changes from flexible single-stranded DNA to rigid double-stranded DNA.

Bis[4-(azidomethyl)phenyl]-1,2-diphenylethene (TPE–2N$_3$) was synthesized following our previous report.[32] TPE–2DNA$_1$ conjugates were synthesized by a click reaction using $CuSO_4$–sodium ascorbate as the catalyst in 1 mL of deionized water and dimethyl sulfoxide (v/v = 1/1). First, freshly prepared sodium ascorbate and copper(II) sulphate aqueous solution were mixed and added into the solvent mixture. The stock solutions of oligonucleotide 5′-alkyne–DNA$_1$ and TPE–2N$_3$ were added subsequently. To optimize the reaction conditions, different amount of $CuSO_4$ (from 100 μM to 1 mM) and sodium ascorbate (from 200 μM to 2 mM) were used and their reaction yields were monitored using HPLC as shown in the Experimental section. It was found that in the presence of 500 μM $CuSO_4$ and 1 mM sodium ascorbate, reaction between 100 μM TPE–2N$_3$ and 250 μM 5′-alkyne–DNA$_1$ led to the maximum yield of around 85%. The retention time of TPE–2DNA$_1$ was measured to be 13.9 min (with absorbance at both 260 nm and 318 nm). Similarly, by conjugation of alkyne–DNA$_2$ and TPE–2N$_3$, TPE–2DNA$_2$ was obtained with a similar retention time of 14.1 min. The *m*/*z* peaks at 12 908.911 and 13 059.224 in MALDI-TOF spectra correspond to the probes of TPE–2DNA$_1$ and TPE–2DNA$_2$, respectively. In this work, both probes were designed to work independently as a sequence-specific DNA probe with AIE characteristics. It is also noteworthy that the two probes TPE–2DNA$_1$ and TPE–2DNA$_2$ consists complementary oligonucleotide DNA$_1$ and DNA$_2$ that can hybridize with each other to form longer stand with tandem repeated units.

We randomly selected TPE–2DNA$_1$ as a representative to study the optical properties and AIE characteristics of the probes. Fig. 1 shows the UV absorption and photoluminescence (PL) spectra of TPE–2N$_3$ and TPE–2DNA$_1$ in DMSO/H_2O solution (v/v = 1/199). Both TPE–2N$_3$ and TPE–2DNA$_1$ have an absorption peak at 318 nm, while TPE–2DNA$_1$ has an additional peak at 260 nm, which corresponds to oligonucleotide absorption. The emission maxima of TPE–2N$_3$ and TPE–2DNA$_1$ are located at 480 nm and 460 nm, respectively. Most importantly, TPE–2DNA$_1$ is almost non-emissive, whereas TPE–2N$_3$ fluoresces strongly (inset of Fig. 1A). As the emission of AIE fluorogens are closely related to the status of molecules, laser light scattering was used to check whether they are dissolved as molecular species or aggregated in aqueous media. As a very hydrophobic AIE fluorogen, TPE–2N$_3$ aggregated with a hydrodynamic diameter around 125 nm, in accordance with its intense fluorescence in aqueous media (Fig. 1B). In contrast, no obvious LLS signal can be detected from the solution of TPE–2DNA$_1$, indicating that the probe is well dispersed in aqueous media. Due to the free intramolecular motion of phenyl rings and the flexibility of oligonucleotide chains, the TPE–2DNA$_1$ shows very weak fluorescence.

It is known that TPE is an iconic AIE fluorogen, which shows weak fluorescence in molecular state but emits strong fluorescence in aggregated state. There have been mechanism studies showing that the excited state energy is consumed through non-radiative pathway to quench the emission by the free rotation of propeller-shaped structures (*e.g.* phenylene rings in TPE).[33,34] On the other hand, when the molecules are aggregated, the radiative decay pathway is activated and strong fluorescence is generated. As the solvent viscosity could affect the intramolecular motion, we used DMSO/glycerol solvents with different volume ratios to study the effect of viscosity on TPE emission. Glycerol is a very viscous liquid having viscosity of 934 cP, which is about 470-fold higher than that of DMSO (1.99 cP) at 25 °C. By varying the ratio of DMSO and glycerol, solvents with different viscosities were obtained. The fluorescence spectra of 10 μM TPE–2N$_3$ in the mixed solvents were

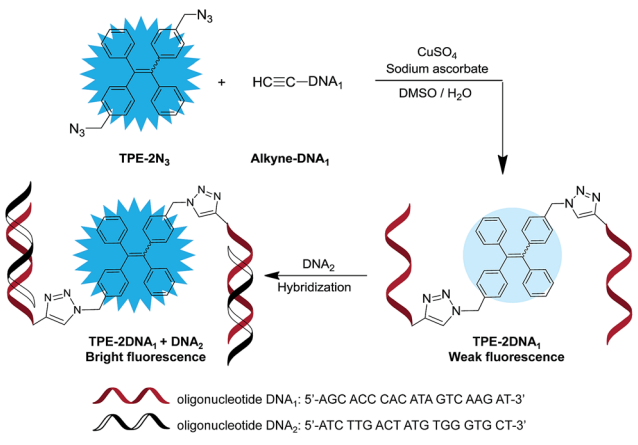

Scheme 1 Synthetic route to TPE–2DNA$_1$ *via* a Cu(I) catalysed "click" reaction and a schematic illustration of its application for nucleic acid hybridization detection. Oligonucleotide DNA$_1$ and DNA$_2$ are complementary to each other and their sequences are shown in the scheme.

collected and the results are shown in Fig. 1C. The peak fluorescence intensities at 480 nm after background removal were found to increase on the semi-log scale with increasing fractions of glycerol from 0% to 99%.

As biosensing is often conducted in buffers and ionic strength can affect the binding behaviour of DNA,[35–37] the effect of ionic strength on the fluorescence of TPE–2DNA$_1$ was studied. The PL spectra of the probe were measured in aqueous solution with different concentrations of NaCl (0–600 mM). As shown in Fig. 1D, the fluorescence intensity of the probe does not change obviously with increasing ionic strength. The result suggests that the probe can be applied to a broad range of ionic strength environment.

The capability of the probe to recognize complementary DNA sequence is examined. Specifically, TPE–2DNA$_1$ hybridized with its complementary strand DNA$_2$ and other strands containing one-base mismatch (DNA$_{M1}$: 5′-ATG TTG ACT ATG TGG GTG CT-3′), two-base mismatches (DNA$_{M2}$: 5′-ATG TTG ACT ATC TGG GTG CT-3′) and a random 20 base pair non-complementary sequence (DNA$_{M3}$: 5′-AGC ATT CAG ATA GTC AAT GT-3′) in PBS buffer and their PL spectra are shown in Fig. 2A. The perfectly matched duplex (TPE–2DNA$_1$ + DNA$_2$) gives much stronger fluorescence over those from mismatched sequences. The duplex (TPE–2DNA$_1$ + DNA$_2$) is about 6.1-fold brighter than that of the probe TPE–2DNA$_1$ alone, showing obvious improvement compared with to one-armed AIE–DNA probe (2.6-fold brighter).[31] In addition, the fluorescence intensities of (TPE–2DNA$_1$ + DNA$_{M1}$) and (TPE–2DNA$_1$ + DNA$_{M2}$) with one or two-base mismatch only increase to 2.1 and 1.8 fold compared to the probe TPE–2DNA$_1$ alone. The fluorescence of the TPE–2DNA$_1$ only shows very small increase towards the random sequence DNA$_{M3}$.

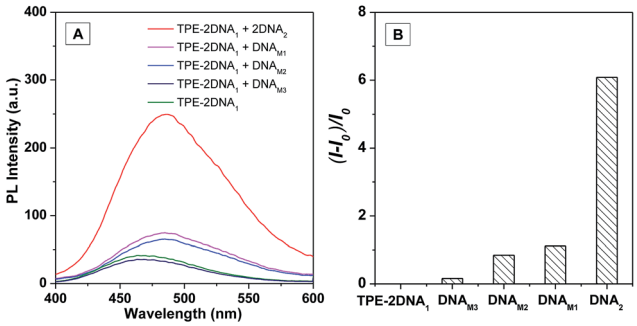

Fig. 2 (A) PL spectra of TPE–2DNA$_1$ alone, and in the presence of complementary DNA$_2$, one-base mismatched single-stranded DNA$_{M1}$, two-base mismatched single-stranded DNA$_{M2}$ and random single-stranded DNA$_{M3}$, (B) fluorescence intensity of the probe in the presence of different DNA strands. I is defined as the maximum fluorescent intensity of each sample, and I_0 is the background fluorescence of TPE–2DNA$_1$ alone (λ_{ex} = 318 nm, [TPE–2DNA$_1$] = 1 μM, [DNA$_2$] = [DNA$_{M1}$] = [DNA$_{M2}$] = [DNA$_{M3}$] = 2 μM).

The ability of both probes (TPE–DNA$_1$ and TPE–2DNA$_1$) to differentiate mutation points was also studied and compared. If we let I_T stand for the PL intensity of the probe upon hybridization with the fully complementary strand while I_{M1}, I_{M2} and I_{M3} represent the PL intensities of the probe hybridized with DNA sequences containing 1, 2 mutation points as well as a random strand. Then $(I_T - I_0)/(I_{M1} - I_0)$ shows the ratio of PL intensity increment of the probe in the presence of the perfect complementary strand over the one-point-mutated sequence. The same calculation was also applied to two-point-mutated sequence and the random sequence and the results are summarized in Table 1. The one-armed probe TPE–DNA$_1$ shows 3.2-fold PL intensity increment upon hybridization with the perfect target sequences over that with one mutation[31] while the ratio becomes 5.5 when the two-armed probe TPE–2DNA$_1$ was employed. The ratios increase to 4.1 and 7.2 for one-armed and two-armed probes in the presence of DNA sequence with two mutation points, respectively. In general, with two oligonucleotides conjugated with TPE core, the probe TPE–2DNA$_1$ becomes more selective to the target sequence.

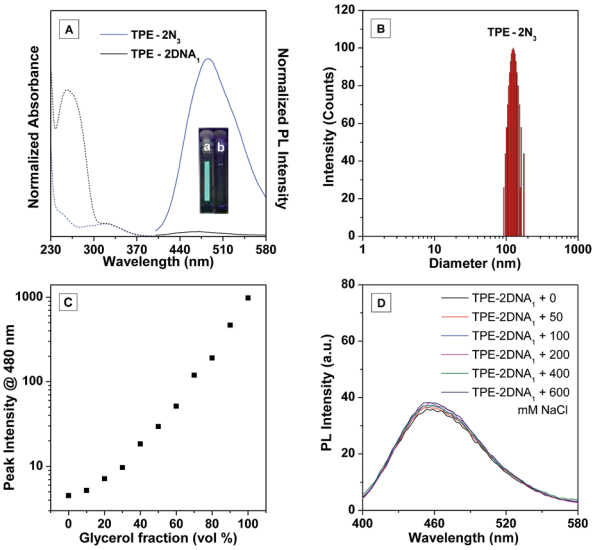

Fig. 1 (A) UV-vis absorption (dotted line) and photoluminescence (PL) spectra (solid line) of TPE–2N$_3$ (blue) and TPE–2DNA$_1$ (black). Inset: photographs of (a) TPE–2N$_3$ and (b) TPE–2DNA$_1$ solution under UV illumination. All the spectra were measured in DMSO/H$_2$O, v/v = 1/199; [TPE–2N$_3$] = [TPE–2DNA$_1$] = 10 μM. (B) Laser light scattering (LLS) measurement of TPE–2N$_3$ aggregates in DMSO/H$_2$O, v/v = 1/199 solution. (C) PL intensity of 10 μM TPE–2N$_3$ at 480 nm *versus* the fractions of glycerol in the mixture of glycerol/DMSO; (D) PL spectra of 1 μM TPE–2DNA$_1$ in aqueous solution in the presence of different concentrations of NaCl (solid line), λ_{ex} = 318 nm.

Table 1 The capability of the probe to differentiate perfectly matched sequence and the sequences with mutation points[a]

	$(I_T - I_0)/(I_{M1} - I_0)$	$(I_T - I_0)/(I_{M2} - I_0)$	$(I_T - I_0)/(I_{M3} - I_0)$
TPE–DNA$_1$	3.2	4.1	29.0
TPE–2DNA$_1$	5.5	7.2	38.1

[a] I_0: PL intensity of the probe alone; I_T: PL intensity of the probe upon hybridization with fully complementary strand; I_{M1}, I_{M2} and I_{M3}: PL intensities of the probe hybridized with DNA sequences containing 1, 2 mutation points as well as a random strand.

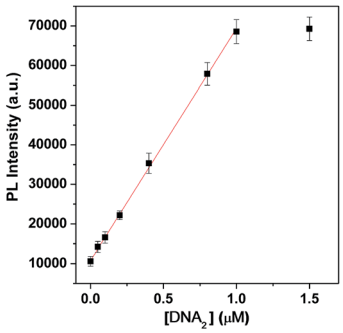

Fig. 3 Fluorescence intensity of TPE–2DNA$_1$ (0.5 μM) in response to different amount of DNA$_2$ (0.05–1.5 μM) in PBS buffer. Error bars are standard deviations of the mean from triplicate measurements.

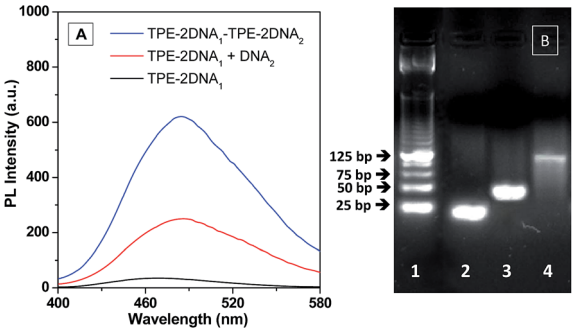

Fig. 4 (A) PL spectra of TPE–2DNA$_1$ (1 μM), duplex with complementary strand (TPE–2DNA$_1$ + DNA$_2$) ([TPE–2DNA$_1$] = 1 μM, [DNA$_2$] = 2 μM), and self-assembled duplex (TPE–2DNA$_1$ + TPE–2DNA$_2$) ([TPE–2DNA$_1$] = [TPE–2DNA$_2$] = 1.0 μM), λ_{ex} = 318 nm. (B) Agarose (4.0%) gel electrophoresis of a 25 bp ladder as standard DNA size marker (lane 1), 20 bp dsDNA (lane 2), duplex (TPE–2DNA$_1$ + DNA$_2$) (lane 3) and the self-assembled duplex (TPE–2DNA$_1$ + TPE–2DNA$_2$, lane 4).

These results prove that the AIE–oligonucleotide conjugation probe has good promise for homogenous sequence-specific detection of DNA and is able to discriminate mutation up to one base. As the double helix structure formed after hybridization could act as a semi-flexible rod-like damper, it restricts the motions of the phenyl structures in TPE and turns on its fluorescence.

To demonstrate the potential of the probe for DNA quantification, 0.5 μM TPE–2DNA$_1$ was titrated with increasing amounts of DNA$_2$ from 0.05 μM to 1.5 μM in PBS buffer. The fluorescence response was recorded in Fig. 3. In the absence of DNA$_2$, the probe TPE–2DNA$_1$ was weakly emissive. With the addition of DNA$_2$ to the probe TPE–2DNA$_1$, the fluorescence increased linearly and it was saturated when DNA$_2$ concentration reached 1.0 μM, showing that the stoichiometric relationship between the probe TPE–2DNA$_1$ and DNA$_2$ is 1 : 2. The detection limit is calculated to be 120 nM.

As illustrated above, the optical property of AIE–2DNA probe is greatly affected by the extent of RIM which results from DNA self-organization. Previously, we have mentioned that the DNA$_1$ and DNA$_2$ are complementary to each other. As a consequence, the mixture of the probe TPE–2DNA$_1$ and TPE–2DNA$_2$ will lead to the formation of a self-assembled duplex (TPE–2DNA$_1$ + TPE–2DNA$_2$), which can further restrict the free motion of TPE as illustrated in Scheme 2.

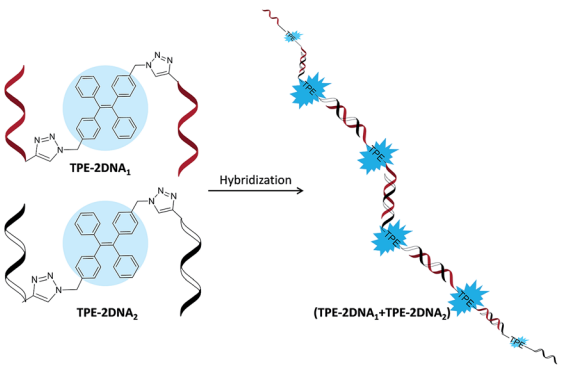

Scheme 2 Schematic diagram of self-assembled duplex (TPE–2DNA$_1$ + TPE–2DNA$_2$) upon hybridization.

To investigate AIE fluorescence enhancement contributed by DNA self-assembly, the PL spectra of TPE–2DNA$_1$, duplex (TPE–2DNA$_1$ + DNA$_2$) and duplex (TPE–2DNA$_1$ + TPE–2DNA$_2$) were measured in PBS buffer solution. Duplex (TPE–2DNA$_1$ + DNA$_2$) and duplex (TPE–2DNA$_1$ + TPE–2DNA$_2$) were prepared containing the same concentration of DNA. Specifically, three samples are (1) 1.0 μM TPE–2DNA$_1$; (2) 1.0 μM TPE–2DNA$_1$ and 2.0 μM DNA$_2$; (3) 1.0 μM TPE–2DNA$_1$ and 1.0 μM TPE–2DNA$_2$, respectively. As shown in Fig. 4, the fluorescence intensity of duplex (TPE–2DNA$_1$ + TPE–2DNA$_2$) is about 2.6 times of the duplex (TPE–2DNA$_1$ + DNA$_2$), although the former only contains 2-fold of TPE as the latter, indicating an obvious increase of fluorescence by controlled AIE through self-assembly of DNA strands. The length of self-assembled duplex (TPE–2DNA$_1$ + TPE–2DNA$_2$) and duplex (TPE–2DNA$_1$ + DNA$_2$) were characterized by agarose (4.0%) gel electrophoresis using a 25 bp DNA ladder as standard size marker in lane 1 (Fig. 4B). The first and second bands from the bottom in lane 1 represent DNA with size of 25 bp and 50 bp, in accordance with the size of 20 bp double-stranded DNA (a reference sample) and the duplex (TPE–2DNA$_1$ + DNA$_2$) (40 bp). The band in the middle of the lane 1 which exhibits brighter illumination stands for the DNA band with size of 125 bp, indicating that the self-assembled duplex (TPE–2DNA$_1$ + TPE–2DNA$_2$, lane 4) consists of about six units of duplex (DNA$_1$–DNA$_2$).

Conclusion

In summary, a two-armed AIE light-up probe was presented for sequence-specific homogenous detection of nucleic acid. By conjugation of alkyne-functionalized oligonucleotides with a bisazide–TPE, the probe shows low background in aqueous solution and fluoresces strongly upon hybridization with its complementary sequence. The probe is able to discriminate sequences with one base pair mutation, showing good selectivity, which is also improved as compared to that for the one-oligonucleotide labelled probe. In addition to hybridization, a self-assembly process can further enhance the AIE fluorescence

of the probe. This AIE–DNA probe is easy to synthesize compared with dual-labelled probe based on FRET or fluorophore/quencher mechanism, low in cost, good tolerance of high ionic strength environment and readily available for a wide range of oligonucleotide sequences.

Experimental section

The chemicals were purchased from Sigma Aldrich, and used directly without further purification. 25 bp DNA ladder was purchased from Life technologies and GelRed *nucleic acid stain* was purchased from Biotium. The oligonucleotides were ordered from Biosearch Technologies, Inc. UV-vis absorption spectra were recorded on a Shimadzu UV-1700 spectrometer. Photoluminescence (PL) spectra were measured on a Perkin Elmer LS-55 equipped with a xenon lamp excitation source and a Hamamatsu (Japan) 928 PMT, using 90 degree angle detection for solution samples. Concentrations of oligonucleotides were determined using Nanodrop TM spectrophotometer at absorbance of 260 nm. All UV-vis absorption and PL spectra were collected at 24 ± 1 °C. The average particle size and size distribution of TPE–$2N_3$ was determined by laser light scattering (LLS) with a particle size analyser (90 Plus, Brookhaven Instruments Co., USA) at a fixed angle of 90 °C at room temperature. HPLC purification was conducted using reverse-phase high-pressure liquid chromatography (HPLC, Shimadzu) on a 250 × 1 mm Kromasil C-18 analytical column connected to a variable wavelength monitor. Phase A is ammonium acetate (50 mmol L^{-1}) buffer; phase B is acetonitrile. MALDI-TOF was conducted using Bruker Autoflux using 3-hydroxypicolinic acid as the matrix.

Synthesis of 1,2-bis[4-(azidomethyl)phenyl]-1,2-diphenylethene (TPE–$2N_3$)

Into a 100 mL round-bottom flask were added 1,2-bis [4-(bromomethyl)phenyl]-1,2-diphenylethene (0.78 g, 1.5 mmol) and sodium azide (0.39 g, 6.0 mmol) in 60 mL of DMSO. After stirring at room temperature overnight, the solution was poured into water and extracted with diethyl ether several times. The organic layer was combined and washed with water and brine, and then dried over $MgSO_4$. After filtration and solvent evaporation, the crude product was purified by a silica gel column using hexane/chloroform (v/v = 2 : 1) as eluent to give TPE–$2N_3$ as a white solid (0.54 g, 82% yield). The final product was characterized by NMR and HRMS. ^{1}H NMR (400 MHz, $CDCl_3$) δ (TMS, ppm): 7.12 (m, 6H), 7.04 (m, 12H), 4.26 (s, 4H). ^{13}C NMR (100 MHz, $CDCl_3$) δ (TMS, ppm): 144.4, 143.9, 141.4, 134.0, 132.4, 131.9, 128.5, 128.4, 128.3, 127.3, 55.2. HRMS (MALDI-TOF), m/z 442.1914 (M^+, calcd 442.1906).

Synthesis of TPE–2DNA conjugates

TPE–DNA was synthesized from alkyne functionalized oligonucleotides with TPE–$2N_3$ by click chemistry. First, 100 nmol TPE–$2N_3$ and 250 nmol alkyne–DNA (DNA_1 (5′-alkyne-AGC ACC CAC ATA GTC AAG AT-3′) or DNA_2 (5′-alkyne-ATC TTG ACT ATG TGG GTG CT-3′)) were mixed in a mixture (1 mL) of deionized water and dimethylsulfoxide (v/v = 1/1). Second, freshly prepared aqueous solution of sodium ascorbate was mixed with copper(II) sulphate and then added into the mixture of DNA and TPE–$2N_3$. The final concentrations of TPE, DNA, copper(II) sulphate, and sodium ascorbate in reaction solution are shown in the following table. The mixture was stirred for 24 h at room temperature before reverse HPLC purification. Quantitative analysis shows an optimized reaction yield of 85.0% (Entry C in the table). After desalination and removing part of water by lyophilization, the TPE–DNA conjugates were obtained as 5 mM stock solutions.

Entry	DNA (μM)	TPE (μM)	$CuSO_4$ (μM)	Sodium ascorbate (μM)	Yield (%)
A	250	100	100	200	25.7
B	250	100	200	400	56.9
C	250	100	500	1000	85.0
D	250	100	1000	2000	42.4

DNA hybridization

All the hybridization was carried out in 1× PBS buffer. 1 mL 1 μM DNA strands were firstly incubated at 70 °C for 3 minutes then slowly cooled down to room temperature and further incubated for two hours before PL measurement.

AIE properties study by varying solvent viscosity

1 μL of 10 mM TPE–$2N_3$ stock solution was first diluted into 999, 899, 799, 699, 599, 499, 399, 299, 199, 99, 9 and 0 μL of DMSO, then 0, 100, 200, 300, 400, 500, 600, 700, 800, 900, and 999 μL of glycerol was added, respectively. After complete mixing, the PL intensity at 480 nm was measured for each sample upon excitation at 318 nm. The background signal of glycerol in each sample was removed by deduction of the PL intensity from blank solvent. Finally, the PL intensity of TPE–$2N_3$ at 480 nm was plotted against the fractions of glycerol in the mixture of glycerol/DMSO.

Detection limit of the probe

The detection limit was calculated based on the fluorescence titration. The fluorescence intensity of the probe TPE–$2DNA_1$ was measured ten times and the standard deviation of blank measurement was obtained. Then the detection limit was calculated with the following equation:

$$\text{Detection limit} = 3\sigma/k$$

where σ is the standard deviation of the blank measurement, k is the slope between the fluorescence intensity *versus* DNA_t concentration. According to the equation, the detection limit for TPE–$2DNA_1$ is deduced to be 120 nM.

Gel electrophoresis of DNA sample

The DNA samples were analysed by electrophoresis in 4.0% (w/v) agarose gel in 1× Tris–borate–EDTA buffer containing Gelred nucleic acid stain. The gel was run for 35 min with voltage fixed at 120 V, then illuminated with a UV

transilluminator and photographed. Lane 1 is 25 bp ladder as standard DNA size marker; lane 2 is a 20 bp double-stranded DNA as reference; lane 3 is the duplex (TPE–2DNA$_1$ + DNA$_2$); lane 4 the self-assembled duplex (TPE–2DNA$_1$ + TPE–2DNA$_2$).

Conflicts of interest

The authors declare no competing financial interest.

Acknowledgements

We thank the Singapore NRF Investigatorship, Ministry of Defence (R297-000-340-232), the SMART (R279-000-378-592), the Research Grants Council of Hong Kong (HKUST2/CRF/10 and N_HKUST620/11) and Guangdong Innovative Research Team Program (201101C0105067115).

Notes and references

1 K. A. Frazer, S. S. Murray, N. J. Schork and E. J. Topol, *Nat. Rev. Genet.*, 2009, **10**, 241–251.
2 J. A. Nicklas and E. Buel, *Anal. Bioanal. Chem.*, 2003, **376**, 1160–1167.
3 H. Ihmels and D. Otto, in *Supermolecular Dye Chemistry*, Springer, 2005, pp. 161–204.
4 B. A. Armitage, in *DNA binders and related subjects*, Springer, 2005, pp. 55–76.
5 C. A. Heid, J. Stevens, K. J. Livak and P. M. Williams, *Genome Res.*, 1996, **6**, 986–994.
6 V. V. Didenko, *Biotechniques*, 2001, **31**, 1106.
7 B. Faltin, R. Zengerle and F. von Stetten, *Clin. Chem.*, 2013, **59**, 1567–1582.
8 W. Tan, K. Wang and T. J. Drake, *Curr. Opin. Chem. Biol.*, 2004, **8**, 547–553.
9 S.-X. Han, X. Jia, J.-l. Ma and Q. Zhu, *Arch. Immunol. Ther. Exp.*, 2013, **61**, 139–148.
10 D. M. Kolpashchikov, *Chem. Rev.*, 2010, **110**, 4709–4723.
11 S. A. Marras, *Mol. Biotechnol.*, 2008, **38**, 247–255.
12 K. Knez, D. Spasic, K. P. Janssen and J. Lammertyn, *Analyst*, 2014, **139**, 353–370.
13 A. A. Martí, X. Li, S. Jockusch, Z. Li, B. Raveendra, S. Kalachikov, J. J. Russo, I. Morozova, S. V. Puthanveettil and J. Ju, *Nucleic Acids Res.*, 2006, **34**, 3161–3168.
14 F. Liang, Y.-Z. Liu and P. Zhang, *RSC Adv.*, 2013, **3**, 14910–14928.
15 B. Liu and G. C. Bazan, *Chem. Mater.*, 2004, **16**, 4467–4476.
16 G. C. Bazan and B. Liu, *US Pat.*, US 8669055 B2, 2014.
17 J. Zhang, S. Song, L. Wang, D. Pan and C. Fan, *Nat. Protoc.*, 2007, **2**, 2888–2895.
18 X. He and N. Ma, *Anal. Chem.*, 2014, **86**, 3676–3681.
19 J. Luo, Z. Xie, J. W. Lam, L. Cheng, H. Chen, C. Qiu, H. S. Kwok, D. Zhu and B. Tang, *Chem. Commun.*, 2001, **18**, 1740–1741.
20 B. Tang, X. Zhan, P. P. S. Lee, Y. Liu and Z. Daoben, *J. Mater. Chem.*, 2001, **11**, 2974–2978.
21 E. P. J. Parrott, N. Y. Tan, R. Hu, J. A. Zeitler, B. Z. Tang and E. Pickwell-MacPherson, *Mater. Horiz.*, 2014, **1**, 251–258.
22 D. Ding, K. Li, B. Liu and B. Z. Tang, *Acc. Chem. Res.*, 2013, **46**, 2441–2453.
23 J. Liang, R. T. K. Kwok, H. Shi, B. Z. Tang and B. Liu, *ACS Appl. Mater. Interfaces*, 2013, **5**, 8784–8789.
24 Y. Hong, C. Feng, Y. Yu, J. Liu, J. W. Y. Lam, K. Q. Luo and B. Z. Tang, *Anal. Chem.*, 2010, **82**, 7035–7043.
25 L. Peng, G. Zhang, D. Zhang, J. Xiang, R. Zhao, Y. Wang and D. Zhu, *Org. Lett.*, 2009, **11**, 4014–4017.
26 H. Shi, R. T. K. Kwok, J. Liu, B. Xing, B. Z. Tang and B. Liu, *J. Am. Chem. Soc.*, 2012, **134**, 17972–17981.
27 H. Tong, Y. Hong, Y. Dong, M. Häußler, J. W. Lam, Z. Li, Z. Guo, Z. Guo and B. Z. Tang, *Chem. Commun.*, 2006, **35**, 3705–3707.
28 M. Wang, D. Zhang, G. Zhang, Y. Tang, S. Wang and D. Zhu, *Anal. Chem.*, 2008, **80**, 6443–6448.
29 Y. Hong, M. Häuβler, J. W. Lam, Z. Li, K. K. Sin, Y. Dong, H. Tong, J. Liu, A. Qin and R. Renneberg, *Chem.–Eur. J.*, 2008, **14**, 6428–6437.
30 M. Wang, G. Zhang, D. Zhang, D. Zhu and B. Z. Tang, *J. Mater. Chem.*, 2010, **20**, 1858–1867.
31 Y. Li, R. T. Kwok, B. Z. Tang and B. Liu, *RSC Adv.*, 2013, **3**, 10135–10138.
32 J. Liang, H. Shi, R. T. Kwok, M. Gao, Y. Yuan, W.-H. Zhang, B. Z. Tang and B. Liu, *J. Mater. Chem. B*, 2014, **2**, 4363–4370.
33 G.-F. Zhang, Z. Q. Chen, M. P. Aldred, Z. Hu, T. Chen, Z. Huang, X. Meng and M. Q. Zhu, *Chem. Commun.*, 2014, **50**, 12058–12060.
34 E. P. Parrott, N. Y. Tan, R. Hu, J. A. Zeitler, B. Z. Tang and E. Pickwell-MacPherson, *Mater. Horiz.*, 2014, **1**, 251–258.
35 P. J. Hagerman, *Annu. Rev. Biophys. Biophys. Chem.*, 1988, **17**, 265–286.
36 C. G. Baumann, S. B. Smith, V. A. Bloomfield and C. Bustamante, *Proc. Natl. Acad. Sci. U. S. A.*, 1997, **94**, 6185–6190.
37 H. Clausen-Schaumann, M. Rief, C. Tolksdorf and H. E. Gaub, *Biophys. J.*, 2000, **78**, 1997–2007.